

APPLICATION OF MATHEMATICAL ABSORBER REFLECTION SUPPRESSION TO DIRECT FAR-FIELD ANTENNA RANGE MEASUREMENTS

Stuart Gregson, Bruce Williams, Gregory Masters, Allen Newell, Greg Hindman
Nearfield Systems Inc.
19730 Magellan Drive,
Torrance, CA 90502-1104

ABSTRACT

Mathematical Absorber Reflection Suppression (MARS) has been used successfully to identify and extract range multi-path effects in a great many spherical [1, 2], cylindrical [3, 4], and planar [5, 6] near-field antenna measurement systems. This paper details a recent advance that enables the MARS measurement and post-processing technique to be used to correct antenna pattern data from far-field or compact antenna test ranges (CATRs) where only a single great circle pattern cut is taken. This paper provides an overview of the measurement and novel data transformation and post-processing chain that is utilised to efficiently correct far-field, frequency domain antenna pattern data. Preliminary results of range measurements that illustrate the success of the technique are presented and discussed.

Keywords: Reflection Suppression, Far-Field, CATR, MARS, Range Length Compensation, Aperture Diagnostics.

1. Introduction

The enduring popularity of the direct far-field antenna range measurement technique is attributable to the ease and simplicity with which asymptotic far-field antenna pattern data can be obtained using relatively simple test equipment. However, the absence of an obligation to undertake intensive mathematical transformations or involved digital signal processing has resulted in a tendency for far-field measurements to receive comparatively little or, in some cases, no additional post-processing. Many of the more sophisticated data post-processing techniques and analyses whose usage have become commonplace when considering near-field antenna measurements are equally applicable and beneficial to direct far-field range measurements. Indeed, in certain circumstances, these can be of even greater utility than in their original area of application. One such example of this is the Mathematical Absorber Reflection Suppression (MARS) technique. This is a frequency domain measurement and post-processing technique which has been used with considerable success in quantifying and subsequently suppressing range multi-path effects in first spherical [1, 2] and then more recently in cylindrical [3, 4] and planar [5, 6] near-field antenna measurement systems. This paper details a recent advance

that, for the first time, enables the MARS technique to be used to correct one-dimensional pattern data for range multi-path effects. Applicable data can be taken using far-field or compact antenna test ranges without recourse to hardware or software time-gating techniques, aggressive aperture plane filtering algorithms, or circular least-squares Argand plane data fitting techniques. MARS processing requires phase information, however many modern direct far-field antenna measurement facilities are equipped with vector network analysers, making the phase data readily available. The acquisition of phase data implies a higher degree of system stability than amplitude-only measurements, although this only need be maintained for the duration of a single cut which can be as brief as a few seconds. The MARS technique is entirely generic in nature, and can be applied to a variety of different antenna types with no *a priori* assumptions being made about the distribution of currents over the antenna under test (AUT).

The following sections provide an overview of the novel measurement and data post-processing chain that is utilised within the far-field MARS (F-MARS) technique which can be extended to include a finite range length correction [7], and an aperture diagnostics capability [8]. Preliminary results of range measurements that illustrate the success of the technique are presented and discussed. Finally, this new far-field implementation is compared and contrasted with the existing MARS implementations.

2. Introduction to Far-Field MARS

Far-field MARS is very closely related to the existing spherical and cylindrical MARS implementations. Spherical MARS has been available for use with far-field ranges and compact antenna test ranges (CATR) for some time, however the existing implementation [1, 2] relies on the acquisition of a complete two dimensional antenna pattern function, *i.e.* $\underline{E}(\theta, \phi)$. Conversely, the F-MARS implementation as introduced here enables MARS processed results to be obtained from only a single one-dimensional far-field pattern cut, *i.e.* $\underline{E}(\phi)$ with θ arbitrary but fixed for the duration of the cut. This is significant, as one of the great strengths of the far-field methodology is its ability to provide a single antenna pattern cut, minimising the required measurement time. Here, a right handed co-ordinate system is used with θ measured from the positive z-axis, ϕ measured from the positive x-axis in

the x - y plane with the antenna being equatorial pointing – which is consistent with conventional cylindrical near-field theory. One of the recognised shortcomings of making single-cut far-field measurements is that range multipath can degrade the accuracy of the measurement results. All versions of MARS require phase *and* amplitude data, however the ability to apply MARS processing to a single cut minimises the measurement duration. This relaxes requirements for thermal and structural stability that may not be possible to achieve over the time needed to take a full two-dimensional raster scan – often the case when using outdoor far-field facilities. An additional requirement is that the acquired far-field great circle pattern data must be tabulated on a monotonic equally spaced angular grid where the sample spacing is dependent upon the frequency and the maximum radial extent (MRE). In this case, the MRE is defined to be the radius of a conceptual cylinder that is centred about the origin of the measurement coordinate system and that is sufficiently large to encompass the majority of the current sources [8, 9, 10].

Typically, an antenna is installed within a near-, or far-field facility such that it is displaced in space as little as possible during the course of a measurement. As range multi-path tends to disturb the fields illuminating the test antenna, the purpose of this strategy is to ensure that the field illuminating the test antenna changes as little as possible during the course of the acquisition, thereby minimising any resulting measurement error. However, the MARS measurement technique deliberately displaces the AUT away from the centre of rotation. This has the effect of making the differences in the illuminating field far more pronounced than would otherwise be the case, and it is exactly this greater differentiation that makes the identification of scattered fields and subsequent removal viable. Clearly, displacing the AUT from the centre of rotation will necessarily increase the MRE and from inspection of equation (1) it is clear that this will correspondingly decrease the angular data point spacing as [8],

$$\Delta\theta = \frac{2\pi}{2(\text{ceil}(k_0\rho_0) + n_1) + 1} \quad (1)$$

Here, *ceil* is used to denote a function that rounds to the nearest integer towards positive infinity, n_1 is a positive integer that depends upon the accuracy required (e.g. $n_1 = 10$ [10]), k_0 is the free-space wave number, and ρ_0 is the MRE. However, as only a single cut is required, the additional data will not typically affect the duration of the measurement providing the measurements are taken on-the-fly and the receiver is sufficiently fast to be able to acquire the data before the next sample point is encountered. Modern VNAs and receivers are sufficiently fast that this should not increase measurement times in all but the most demanding multiplexed applications where a

great many frequencies and or beam states are acquired. Displacing the AUT in this way also has an implication for the Rayleigh far-field criterion [8] since this can also be expressed in terms of the MRE. It can also be seen that increasing the MRE will similarly increase the required range length, *i.e.* the minimum required separation between the AUT and the remote source antenna [8] as,

$$R = \frac{2D^2}{\lambda} \approx \frac{2(2\rho_0)^2}{\lambda} = \frac{8\rho_0^2}{\lambda} \quad (2)$$

Once a far-field great circle pattern cut has been acquired, with the measurement adhering to equations (1) and (2), the AUT has to be mathematically translated back to the origin of the measurement coordinate system by means of a differential phase change [8],

$$\underline{E}_i(r \rightarrow \infty, \theta, \phi) = \underline{E}(r \rightarrow \infty, \theta, \phi) e^{j\mathbf{k}_0 \cdot \underline{r}} \quad (3)$$

Here, \underline{r} denotes the displacement vector between the centre of the measurement coordinate system and the centre of the current sources e.g. the aperture of the AUT. In the true far-field this expression is exact. However, for the case of a measurement taken at a large but finite range length where the separation is sufficiently large to satisfy the far-field condition, this relation still remains a very good approximation. This mathematical translation has the effect of reducing the number of mode coefficients, of any elementary kind, that are required to represent the far-field pattern. The equivalent cylindrical mode coefficients (CMCs) can be obtained from far electric fields using standard cylindrical near-field theory [3, 4],

$$B_n^1(\gamma) = -\frac{(-j)^{-n}}{4\pi\kappa} \int_0^{2\pi} E_\phi(r \rightarrow \infty, \theta, \phi) e^{-jn\phi} d\phi \quad (4)$$

$$B_n^2(\gamma) = -j \frac{(-j)^{-n}}{4\pi\kappa} \int_0^{2\pi} E_\theta(r \rightarrow \infty, \theta, \phi) e^{-jn\phi} d\phi \quad (5)$$

Here, ϕ represents a rotation about the vertical axis while θ is measured away from the positive vertical axis. The additional factor of 2π is introduced in the denominator of equations (4) and (5) to enforce the correct normalisation of the CMCs, *c.f.* equations (7) and (8). For a fixed measurement radius and frequency, these mode coefficients are complex numbers that do not vary with any of the scanning coordinates and are instead functions of n the angular index, and γ the Fourier variable which is the conjugate of the linear spatial variable z , such that $-\infty \leq n \leq \infty$, $-\infty \leq \gamma \leq \infty$. Strictly, equations (4) and (5) are only valid in the true far-field. However, providing the measurements are taken with a finite but sufficiently large range length that guarantees the far-field condition is satisfied [8], then these integrals may be used with a high degree of confidence. Similarly, probe pattern correction [9] can be effectively ignored since in the far-field the maximum radial extent only subtends a very small angular range as seen from the remote source antenna [10]. That is, the probe (remote

source antenna) pattern is effectively constant over the sphere containing the AUT that is centred about the origin of the measurement coordinate system.

From examination of equations (4) and (5), it is clear that for a fixed value of θ it is possible to deduce all CMCs for a corresponding value of γ . It is this observation that allows the MARS technique to be extended and applied to one-dimensional far-field applications as when processing great circle far-field cuts, where the polar angle $\theta = \pi/2$ radians. From inspection of equations (4) & (5), and (7) & (8) it is clear that the TE and TM CMCs are uncoupled from one another and that the θ and ϕ -polarised electric fields are also uncoupled from one another. Crucially, this enables far-field MARS processing to be applied to only a *single* far electric field component. Thus, dual polarised acquisitions are not required in all instances, cutting measurement time in half when cross-polar pattern information is not required. Strictly, as only far-field applications are being considered, only a single value of γ is used and this dummy variable (together with its Fourier conjugate variable z) can be omitted from the notation. Its retention here is merely intended to show how this application relates to the more general, and very well established, cylindrical formulation [9].

Once the cylindrical mode coefficients for the (now ideally centrally located) AUT have been recovered, any mode representing fields outside the ideal conceptual minimum MRE (r_{10}) can be filtered out, removing contributions that are not associated with the AUT. Thus, from standard cylindrical theory [3, 4, 9], it is possible to filter out all higher order modes without affecting the integrity of the underlying antenna pattern function. When expressed mathematically the band-pass brick-wall mode filter function can be expressed as,

$$B_n^s(\gamma) \Big|_{s=1,2} = \begin{cases} B_n^s(\gamma) & n^2 + (\gamma r_{10})^2 \leq (k_0 r_{10})^2 \\ 0 & \text{elsewhere} \end{cases} \quad (6)$$

Here, it is clear that the CMCs associated with the AUT are confined to a narrow band that are tightly distributed about the $n = 0$ coefficient. As the total power radiated by the AUT must be conserved, the amount of power per mode must increase as the total number of modes associated with the AUT decreases. As the amount of noise per mode can be seen to be roughly constant with respect to the maximum level, the effective system signal to noise (SNR) ratio of the measurement is significantly increased. Crucially, and as has been observed previously with *all* other MARS implementations, although the AUT has been translated back to the origin of the measurement coordinate system, this is not the case for the scatterers which are spatially extended and are represented by many *higher* order modes. In effect, the contributions in the CMC domain of the AUT and the scatterers are separated so that they do not interfere and are in essence

orthogonalised from one another. The MARS processed asymptotic far-field pattern can be obtained from a simple summation of CMCs as [3, 4, 9],

$$E_\theta(r \rightarrow \infty, \theta, \phi) = 2jk_0 \sin \theta \sum_{n=-\infty}^{\infty} (-j)^n B_n^2(\gamma) e^{jn\phi} \quad (7)$$

$$E_\phi(r \rightarrow \infty, \theta, \phi) = -2k_0 \sin \theta \sum_{n=-\infty}^{\infty} (-j)^n B_n^1(\gamma) e^{jn\phi} \quad (8)$$

$$E_r(r \rightarrow \infty, \theta, \phi) = 0 \quad (9)$$

Thus the complete electromagnetic six-vector can be computed in the far-field as the waves are transverse and the electric and magnetic fields are orthogonal [8],

$$\underline{H}(\theta, \phi) = \frac{\hat{e}_r \times \underline{E}(\theta, \phi)}{Z_0} \quad (10)$$

Here, per the usual convention, the unimportant far-field spherical phase factor and inverse r term have been suppressed. As these transforms and their inverse operations can be evaluated using the one dimensional fast Fourier transform (FFT) this makes the F-MARS algorithm very efficient in terms of computational effort and resources. In summary, the F-MARS algorithm can be described as follows:

1. Take a direct acquisition of the one-dimensional far electric field amplitude and phase pattern functions with the AUT offset from the origin.
2. Apply a differential phase change to mathematically translate the AUT to the origin of the measurement coordinate system.
3. Obtain the translated mode coefficients of the AUT for an AUT conceptually located at the origin of the measurement coordinate system.
4. Apply band pass mode filtering function to suppress unwanted higher order CMCs where the properties of the filter function are determined from the physical size of the AUT and the free space propagation number.
5. Compute the complete far electric field pattern from the filtered mode coefficients to obtain the MARS filtered AUT pattern function.

3. Preliminary Measured Results

In order that this new measurement and post-processing technique could be verified, a far-field measurement range was constructed and used to measure the quasi-far-field pattern of a C-band standard gain horn (SGH) in an environment subject to severe multipath reflections. For this experiment, an NSI-700S-20 spherical near-field scanner was used with an auxiliary far-field source antenna and some additional structural members to provide far-field cuts with a wide selection of AUT offsets. This system can be seen presented in Figure 1 below. The antenna under test (AUT) was a NARDA WR-137 gain horn with an E-plane aperture of 4.5 inches (horizontal-axis) and an H-plane aperture of 6 inches

(vertical-axis) transmitting at 5 GHz. A medium gain AUT was chosen so that multiple reflections would be clearly evident on the measured far-field pattern. The “far-field” source antenna was an NSI-RF-SG137 standard gain horn, located 25 feet from the AUT axis of rotation. The NSI-700S-20 scanner allows for AUT motion on a “model tower” positioner. For these tests, the upper “roll” axis was fixed with only the lower axis being moved thereby allowing single (horizontal) polarisation azimuth cuts to be taken. The source horn was similarly horizontally polarised, providing co-polarised measurements only. An Agilent 8720 vector network analyser (VNA) was used with the scanner to provide amplitude and phase measurements at 1° sample spacing on 360° azimuth cuts. As can be seen from the photograph shown in Figure 1, the range was situated in an open factory floor environment with plenty of opportunities for multipath reflections to corrupt the measured patterns.

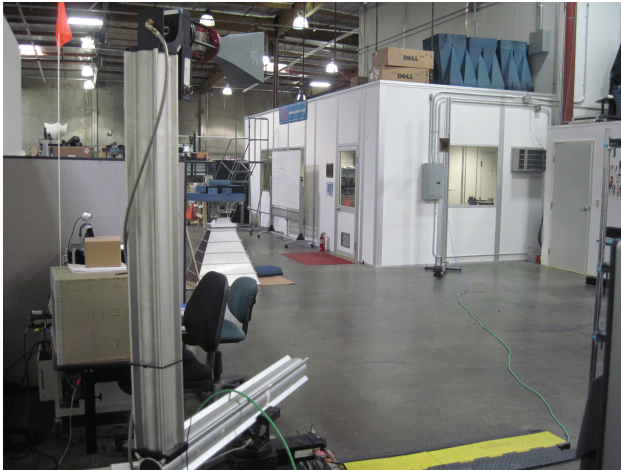


Figure 1 – NSI-700S-20 far-field antenna measurement system in a multipath-rich environment. The AUT is visible to the upper left of the picture mounted on the model-tower positioner. The remote source antenna is in the upper right quadrant of the photo, above and to the right of an electrical panel.

Data were taken for the AUT with the aperture at several different offsets from the origin of the measurement coordinate system, to illustrate the effect of the offset on the CMCs, and thus on the MARS correction. Figures 2, 4, and 6 show the measured far-field patterns (red trace) plotted together with the MARS filtered equivalent plots (blue trace) for the cases where the AUT was displaced by 0”, 8” and 16” respectively. In these plots ϕ is used to denote the azimuthal angle. Figures 3, 5, and 7 contain the equivalent CMC plots with (blue trace) and without (red trace) MARS filtering as described by equation (6). It can be seen that in the zero-offset case, the multipath and AUT modes are coincident, and thus MARS processing provides virtually no pattern correction. In the case where the offset is 8 inches (greater than the antenna conceptual minimum MRE) it is

clear that the multipath CMCs can now be clearly resolved from the antenna coefficients, which are closely distributed about the lowest order mode. Here, MARS processing starts to reveal sidelobe details in the AUT pattern. Finally, the 16-inch case shows coefficients fully resolved, offering a clear view of the AUT pattern including the sidelobes. The observed suppression of range multipath effects (about 20 dB) is very comparable with the typical improvement obtained from the cylindrical MARS technique. Note that as the offset is increased, the spectral peak representing multipath energy tends to move further away (towards higher order mode numbers) from the AUT spectral peak (shown in the centre of the plot at $n = 0$). Also, note that the multipath spectrum becomes wider as the offset is increased.

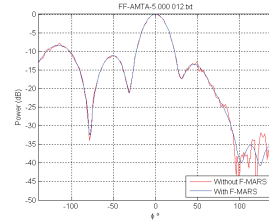


Figure 2 – Azimuth ϕ cut with and without MARS processing. Displacement of 0”.

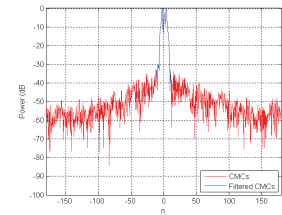


Figure 3 – Equivalent CMCs for displacement of 0”.

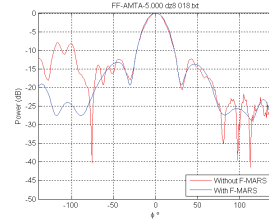


Figure 4 – Azimuth ϕ cut with and without MARS processing. Displacement of 8”.

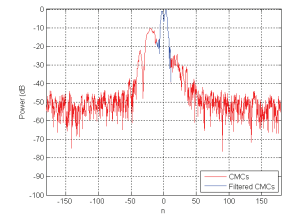


Figure 5 – Equivalent CMCs for displacement of 8”.

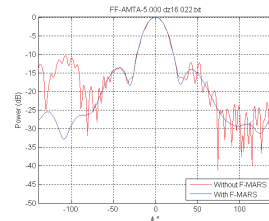


Figure 6 – Azimuth ϕ cut with and without MARS processing. Displacement of 16”.

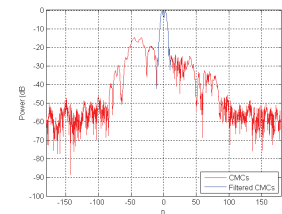


Figure 7 – Equivalent CMCs for displacement of 16”.

The displacement of the spectral peak of the scatterers to increasingly higher order modes with increasing AUT offset corresponds with a change in the appearance of the measured far-field patterns. Sidelobe ripple in the uncorrected patterns (red traces in Figures 2, 4, and 6) tends toward higher angular frequency as the AUT offset increases. This ripple is a result of the direct and indirect (scattered) signals adding in and out of phase as the AUT is rotated. Clearly, the further the AUT is displaced across the range quiet zone during the measurement, the more rapidly the signals will beat in and out of phase and

the higher the angular frequency of the resulting ripple will be observed on the measured antenna pattern. This correlates with the observed movement of the multipath mode energy into higher-order modes – the separation between the AUT and the multipath patterns becomes more obvious in both domains.

The conceptual minimum MRE which is used by the MARS CMC filter function to exclude scattering from the measurements must be sufficiently large to create a conceptual cylinder that is coaxial with the rotation axis and which circumscribes the majority of the current sources. As the AUT was a medium-gain SGH which was acquired in the E-plane, significant currents flow down the vertical exterior surfaces of the exponential horn. For this reason, this horn is not a true aperture antenna as the excitation current distribution extends in all three Cartesian axes. These fields contribute to the far-field pattern, particularly to the wide angle sidelobes, and therefore should *not* be excluded from the measurement by the F-MARS processing. Thus, a conservative radius of 4.5” was employed (which was larger than the width of the aperture) as this retained these exterior fields.

Although the computation of the CMCs (as shown in Figures 3, 5 and 7) is implemented through the use of an efficient FFT algorithm, far-field MARS processing does *not* attempt to reconstruct a spatial aperture illumination function via the plane-wave spectrum, *c.f.* [5]. Thus, far-field MARS processed far-field pattern data is available over a complete 360° great circle cut and is not limited to merely a 180° half-space. The far-field distance for these three measurements was estimated using equation (2) which indicated that only the 16” offset measurement was taken with a range length that was slightly too short to be in the true far-field. However, the measured pattern contains a good approximation of the true far-field pattern with finite range length correction techniques being well documented in the open literature, *e.g.* [7].

4. Summary and Future Work

Far-field MARS processing can be used with a very high degree of confidence since all the steps in the measurement and analysis are consistent with the well-established principles of the standard cylindrical near-field theory and measurement technique, and all comparisons to date have proved overwhelmingly positive. The offset of the AUT and the resulting smaller data point spacing are valid if the data point spacing satisfies the sampling criteria. The translation of the far-field pattern to the origin with the application of a differential phase change is rigorous. The selection of the mode cut-off for the translated pattern is based on the physical dimensions of the AUT and its translated location. The results of the processing will reduce, but not entirely eliminate, the effect of the scattering. The final result with MARS processing can be degraded if the

sampling of the measured data is too coarse, or the mode filter is too tight, *i.e.* abrupt and importantly, both of these parameters are controlled by the user. This frequency domain measurement and processing technique is very general and can be used to achieve acceptable results with use of minimal absorber or even without the use of an anechoic chamber. It can also improve the reflection levels in a traditional anechoic chamber or outdoor facility allowing improved accuracy as well as offering the ability to use existing facilities where spurious scatters cannot be readily removed or suppressed using other techniques.

It should be noted that this paper recounts the progress of an ongoing research study. Consequently, several issues remain to be addressed and the planned future work is to include obtaining further verification of the success of the far-field MARS technique using a CATR, and through computational electromagnetic (CEM) simulation of a reflection-contaminated far-field measurement.

5. REFERENCES

- [1] G.E. Hindman, A.C. Newell, “Reflection Suppression in a large spherical near-field range”, AMTA 27th Annual Meeting & Symposium, Newport, RI, October. 2005.
- [2] G.E. Hindman, A.C. Newell, “Reflection Suppression To Improve Anechoic Chamber Performance”, AMTA Europe 2006, Munich, Germany, March 2006.
- [3] S.F. Gregson, A.C. Newell, G.E. Hindman, “Reflection Suppression in Cylindrical Near-Field Antenna Measurement Systems – Cylindrical MARS”, AMTA 31st Annual Meeting & Symposium, Salt Lake City, UT, November 2009.
- [4] S.F. Gregson, A.C. Newell, G.E. Hindman, M.J. Carey, “Advances in Cylindrical Mathematical Absorber Reflection Suppression”, 4th European Conference on Antennas and Propagation, Barcelona, 12th - 16th April, 2010.
- [5] S.F. Gregson, A.C. Newell, G.E. Hindman, M.J. Carey, “Extension of The Mathematical Absorber Reflection Suppression Technique To The Planar Near-Field Geometry”, AMTA, Atlanta, October 2010.
- [6] S.F. Gregson, A.C. Newell, G.E. Hindman, M.J. Carey, “Application of Mathematical Absorber Reflection Suppression to Planar Near-Field Antenna Measurements”, 5th European Conference on Antennas and Propagation, EuCAP 2011, Rome, April 2011.
- [7] G.E. Evans, “Antenna Measurement Techniques”, Artech House, 1990.
- [8] S.F. Gregson, J. McCormick, C.G. Parini, “Principles of Planar Near-Field Antenna Measurements”, The Institution of Engineering and Technology, UK, 2007.
- [9] A.D. Yaghjian, “Near-Field Antenna Measurements On a Cylindrical Surface: A Source Scattering Matrix Formulation”, NBS Technical Note 696, 1977.
- [10] J.E. Hansen (ed.), “Spherical Near-Field Antenna Measurements”, IET, UK, Peter Peregrinus Ltd., 1988.

6. ACKNOWLEDGMENTS

The authors wish to thank Mr S.C. Jones for his assistance in constructing the test range, verifying the test equipment, and acquiring preliminary data in preparation for the work presented here.